TÜBİTAK

Turkish Journal of Physics

http://journals.tubitak.gov.tr/physics/

Research Article

Turk J Phys
(2018) 42: 223 – 231

doi:10.3906/fiz-1711-4

Density functional theory of cubic zirconia and 6–15 mol% doped yttria-stabilized zirconia: structural and mechanical properties

Berna AKGENÇ[1,*], **Tahir ÇAĞIN**[2]

[1]Department of Physics, Faculty of Science, Kırklareli University, Kırklareli, Turkey

[2]Department of Material Science and Engineering, Texas A&M University, College Station, Texas, USA

Received: 02.11.2017 • **Accepted/Published Online:** 23.01.2018 • **Final Version:** 26.04.2018

Abstract: Results of ab-initio density-functional theory calculations within the generalized gradient approximation (GGA-PBE) of structural and mechanical properties of cubic zirconia and yttria-stabilized zirconia (YSZ) with yttria (Y_2O_3) concentrations of 6.67, 10.34, and 14.28 mol% are reported. It is found that the calculated structural and mechanical parameters of all considered structures are highly consistent with the existing experimental data and the other theoretical values. The doping concentration of yttria-stabilized zirconia has critical importance in ionic conductivity and stabilization of high temperature down to room temperature. The lattice parameter and cell volume linearly decrease with increases in doping concentration. Moreover, the effects of doping of yttria-stabilized zirconia on elastic constants are studied. Elastic constants of cubic zirconia and 6–15 mol% doped yttria-stabilized zirconia are calculated using the strain-stress approach and linear response theory.

Key words: First-principle calculations, DFT, structural properties, mechanical properties, cubic zirconia, yttria-stabilized zirconia

1. Introduction

Renewable energy plays an important role in providing sustainable energy to meet demand. Fuel cell technology has been gaining popularity amongst renewable energy technology in recent years [1–3]. A fuel cell is an electrochemical device that converts electricity from a chemical reaction. Fuel cells have some advantages; to name a few: their significant environmental benefits, high efficiency converting chemical energy into usable form, and hence expanding the alternatives of providing sustainable energy to meet demand [4]. Solid oxide fuel cells (SOFCs) are quite likely to become commercially viable among fuel cell technologies because of operating at intermediate temperature (400–700 °C). SOFCs use a solid ceramic electrolyte, such as stabilized yttria zirconia, instead of a liquid or membrane. Zirconium oxide (ZrO_2) is known, as zirconia has been of great scientific and technological material interest in gas sensors, high-temperature electrolysis, thermal barrier coatings, solid oxide fuel cells, etc. ZrO_2 exists in three phases: monoclinic zirconia at temperatures less than 1170 °C, tetragonal from 1170 °C to 2370 °C, and cubic from 2370 °C to 2680 °C polymorphs at ambient pressure [5]. The highest ionic conductivity has been shown in the cubic phase [6]. Cubic zirconia can be stabilized by addition of aliovalent oxides such as Y_2O_3 at ambient temperature. The addition of yttria to pure zirconia replaces some Zr^{+4} ions with Y^{+3} ions that create charge compensating oxygen vacancies for balancing the valence charge.

*Correspondence: berna.akgenc@klu.edu.tr

In Kröger–Vink notation:

$$\boldsymbol{R_2O_3} \xrightarrow[\boldsymbol{ZrO_2}]{} \boldsymbol{2R'_{Zr} + V_{\ddot{O}} + 3\,O_O^x} \tag{1}$$

where R represents the doping Y^{+3}.

The oxygen vacancies make it possible for oxygen ions to move through the electrode by hopping from vacancy to vacancy in the lattice. The amount of yttrium in YSZ not only affects the crystal structure and but also influences the transport properties of the material.

Several works have investigated the structural, mechanical, and thermodynamic properties of cubic ZrO_2 [7–9]. Cousland et al. have studied electronic and vibrational properties of three phases of ZrO_2 and yttria-stabilized zirconia using first-principle methods for 10–40 mol% Y_2O_3. They have observed that yttria doping of zirconia results in a smaller valence bandwidth and a larger band-gap [10]. Pomfret et al.'s work is also on the structural and compositional properties of YSZ, where they have discussed how the compositions of electrolytes affect electrochemical operation [11].

Liang et al. have shown that PBE and PW91 ultrasoft pseudo-potentials that they used to calculate the structural, mechanical, and thermodynamic properties are more accurate than the local density approximation (LDA). Hence, we employed PBE potential throughout this study [12]. Nain et al. calculated total energy as a function of crystal volume for yttria with three different fittings to the equation of state (EOS): a fourth-order polynomial, Murnaghan, and Birch–Murnaghan EOS. They have concluded that the result based on the Birch–Murnagham EOS is more accurate amongst the 3 forms, especially for B‘ [13].

The aims of the present study were to systematically investigate structural and mechanical properties of the cubic form of ZrO_2 and different concentrations of Y_2O_3 doped yttria-stabilized zirconia.

2. Calculation methods

The first-principles calculations are performed by the Vienna ab-initio simulation package program (VASP), based on density functional theory (DFT) with the generalized gradient approximation (GGA) using a plane-wave basis set [14]. We have started with calculating the structural properties of the cubic form of ZrO_2. The Zr^{+4} atoms have been described by twelve ($4s^2\,4p^6\,4d^2\,5s^2$), Y^{+3} atoms by eleven ($4s^2\,4p^6\,4d^1\,5s^2$), and O^{-2} atoms by six ($2s^2\,2p^4$) valence electrons, respectively. Kinetic energy cut-off for plane waves, 600 eV, and a $\boldsymbol{4x4x4}$ k-point mesh for the total energy calculations have been determined as optimized values. The Monkhorst–Pack method is used for k-mesh. The geometrical relaxation calculations are also performed with the following common parameters: convergence criterion for energy is $\boldsymbol{10^{-5}eV}$; the convergence criterion for the maximal force between the atoms is 0.005 eV/Å; the maximum ionic steps are 200. The crystal structure of the cubic form of ZrO_2 is the calcium fluoride structure with space group *Fm3m* (space number 225). It is based on the fcc lattice and basis with Zr atom (0,0,0) and O's at (0.25,0.25,0.25) and (0,75,0.75,0,75) to generate 4 formula units of ZrO_2 in the primitive unit cell. The conventional bulk cell of the fluorite structure consists of four zirconium and eight oxygen ions. Yttria stabilized zirconia (YSZ) is generated by starting with the cubic form of ZrO_2 in Figure 1.

The doped yttria on cubic zirconia not only results in high ionic conductivity but also in the stabilization of the high-temperature fluorite structure down to ambient temperature. To get doped 6–15 mol% yttria of zirconia, we have studied several sizes of super cells: 2 × 1 × 1 (Model 1- 24 atoms), 2 × 2 ×1 (Model 2- 48 atoms) and 2 × 2 × 2 (Model 3- 96 atoms). The addition of yttria to the pure zirconia for each

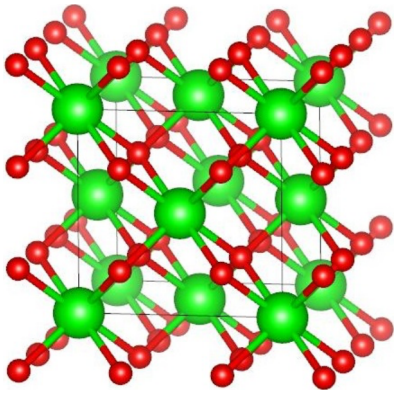

Figure 1. The crystal structure of cubic fluorite phase of zirconia.

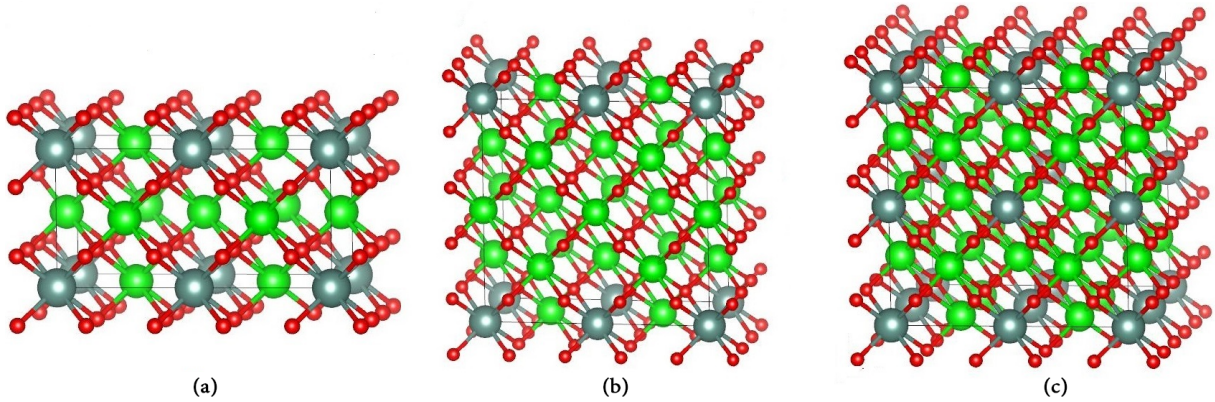

Figure 2. The crystal structure of 14.28 mol% Y_2O_3 doped YSZ for 2 × 1 × 1 (a), 6.67 mol% Y_2O_3 doped YSZ for 2 × 2 × 1 (b), 10.34 mol% Y_2O_3 doped YSZ for 2 × 2 × 2 (c).

concentration is performed by replacing an appropriate number of Zr^{+4} ions with an appropriate number of Y^{+3} ions. To satisfy the charge neutrality of the crystal for the stoichiometry generated, the oxygen vacancies are introduced by deleting the appropriate number of oxygen. Yttria (Y_3O_2) has a cubic structure of space group *Ia3-(* $\boldsymbol{T_h^7}$) (space number 225) that contains two nonequivalent cation sites with a lattice parameter of 10.604 $\boldsymbol{\mathring{A}^3}$. Moreover, 14.28 mol% yttria $Y_2Zr_6O_{15}$, 6.67 mol% yttria $Y_2Zr_{14}O_{31}$, and 10.24 mol% ytria $Y_6Zr_{26}O_{61}$ are created from 2 × 1 × 1, 2 × 2 × 1 and 2 × 2 × 2 supercells, respectively (see Figure 2).

The initial lattice parameters of these supercells are initially chosen according to Vegard's rule. Basically the rule can be applied by the following formula:

$$\boldsymbol{a_{YSZ}=x\,a_{Y_2O_3}+(1-x)\;a_{ZrO_2}} \tag{2}$$

The ionic relaxation is performed and the equilibrium volume of the primitive cell is calculated at zero pressure for all structures and configurations.

The structure of 2 × 1 × 1 supercell is created by two Y^{+3} ions interstitially replaced by two Zr^{+4} ions with one oxygen vacancy. According to 14.28 mol% yttria concentration of 24 atoms for 2 × 1 × 1 unit cell, all the possible configurations could easily be studied ($\frac{\mathbf{8!}}{\mathbf{6!2!}}$ 28 different configurations, 8 different interstitial sites for 2 yttrium atoms). We have found the configuration that gives the minimum energy among

all possible configurations. We have calculated structural and mechanical properties for the configuration that gives the minimum energy. With increasing number of supercells as 2 × 2 × 1 and 2 × 2 × 2 supercells, the possible configurations of yttrium atoms in the crystal is hard to calculate. We have randomly created oxygen vacancy for the rest of the crystal structures. Because of the limitation of atom numbers of quantum chemistry calculations, increasing number of atoms in supercells is balanced by reducing the number of k-point sampling. For optimal computational accuracy and efficient use of computational resources, we have performed 2 × 2 × 2 k-point sampling for 2 × 2 × 2 supercell.

3. Results

3.1. Structural properties

The calculated total energies as a function of a primitive cell volume (12 atoms) for the cubic fluorite phase of zirconia and 6–15 mol% Y_2O_3 on cubic zirconia are used to determine structural and mechanical properties by a least-squares fit of third-order Birch–Murnaghan equation, which is given as [12]

$$E(V) = E_0 + \frac{9V_0B_0}{16}\left\{\left[\left(\frac{V_0}{V}\right)^{2/3} - 1\right]^3 B_0' + \left[\left(\frac{V_0}{V}\right)^{2/3} - 1\right]^2 \left[6 - 4\left(\frac{V_0}{V}\right)^{2/3}\right]\right\}, \quad (3)$$

where E0 is the total energy, V0 is the equilibrium volume, B0 is the bulk modulus at 0 GPa pressure, and B_0' is the first derivative of bulk modulus with respect to pressure in Figure 3.

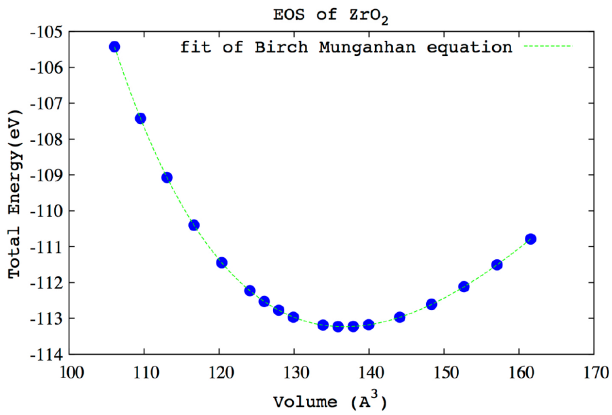

Figure 3. Total energy as a function of conventional cell volume (12 atoms) for cubic fluorite phase of zirconia from ab-initio calculations. The calculated values are shown by circles. The dashed line represents the fit of the data to the Birch–Munganhan EOS.

Table 1 shows the structural parameters obtained after the fitting procedure with respect to pressure at 0 GPa. It also shows the calculated equilibrium energy (E_0 in eV), the lattice parameters (a in $\AA$), the bulk modulus B in GPa, the pressure derivative of bulk modulus B‘, the Zr–O distance (d_{Zr-O} in $\AA$), and the Y–O distance (d_{Y-O} in $\AA$) after relaxation. We find the lattice constant of pure zirconia to be 5.15 $\AA$, which is very close to the experimental value of 5.09 $\AA$ within the GGA-PBE approximation.

Vacancies or dopant/substitution atoms have critical importance in material properties for YSZ. While substituent Y atoms decrease over all positive charge in the cubic form of zirconia, through the introduction of oxygen vacancy models maintain charge neutrality. As the oxygen vacancies prefer to be close to the smallest

Table 1. The calculated structural parameters of cubic zirconia and 6–15 mol% doped yttria-stabilized zirconia.

Structure	E_0 (eV)	V_0 ($\AA^3$)	a ($\AA$)	B (GPa)	B‘	d_{Zr-O} ($\AA$)	d_{Y-O} ($\AA$)
ZrO_2	–113.23	136.72	5.15	233.44	4.26	2.21	-
	–91.80[c]	129.97[d]	5.07[a] 5.14[c]	209[b] 228[c]	4.43[e]	2.19[d]	-
$Y_2Zr_{14}O_{31}$ (6.67 mol%)	–111.52	140.39	5.19	151.08	5.96	2.97	2.41
$Y_6Zr_{26}O_{61}$ (10.24 mol%)	–110.11	141.08	5.20	155.68	5.67	2.88	2.56
$Y_2Zr_6O_{15}$ (14.28 mol%)	–108.42	141.36	5.21	14 1.44	6.15	2.42	2.48
[a]Ref [15], [b]Ref [16], [c]Ref [10], [d]Ref [17], [e]Ref [18]							

cation because of smaller Pauling radius (since Zr^{+4} has a Pauling radius of 0.80 Å and Y^{+3} of 0.93 Å, respectively), the distance of cation atom (Zr, Y) and oxygen atom (O) decreases. Replacing Zr atom with Y atom leads to an increase in volume of the cell at ground state. Since the atomic radius of yttrium and zirconium is larger than the atomic radius of oxygen, distances of d_{Zr-O} and d_{Y-O} can change with creating oxygen vacancy.

3.2. Mechanical properties

The bulk materials respond to application of stress by changing their form, size, or both. The change can be described by elastic properties. The elastic properties are also the key component for describing mechanical properties. There are two main approaches that can be used to obtain the elastic constants from first-principle calculations. The linear response theory (LRT) is used to represent how a system reacts to external influences like applied pressure/stress. Finite strain continuum elastic theory is related to the analysis of the total calculated energy of a crystal as a function of applied strain [19]. In the present study, we have calculated elastic constants with these two methods, presented in Table 2.

Table 2. The calculated elastic constants (C_{ij} in GPa) for cubic zirconia with available theoretical calculations and experimental measurements.

C_{11}	C_{12}	C_{44}	B	G	E	υ	Method
553.55	124.79	71.07	267.71	112.7	296.49	0.37	LRT
528.70	122.94	97.98	258.19	131.73	337.74	0.28	Cont. theory
545.13[c]	103.72[c]	72.66[c]	250.85[c]	109[b]	283[b]	0.29[b]	Theo.
401.00[a]	96.00[a]	60.00[a]	197.66[a]				Exp.
[a]Ref [20], [b]Ref [12], [c]Ref [17]							

In accordance with finite strain continuum elastic theory, the deformation corresponding to small strain is imposed on a model crystal in a linear elastic manner. The calculated energy of the strained system may then be expressed by a Taylor series expansion in terms of strain as follows:

$$E(V,\varepsilon) = E(V_0,0) + V_0 \sum_{i=1}^{6} \sigma_i \varepsilon_i + \frac{1}{2!} V_0 \sum\nolimits_{i,j=1}^{6} C_{ij} \varepsilon_i \varepsilon_j + \frac{1}{3!} V_0 \sum\nolimits_{i,j,k=1}^{6} C_{ijk} \varepsilon_i \varepsilon_j \varepsilon_k, \quad (4)$$

where ε and σ are the strain and stress tensors, respectively. $E(V_0\,,0)$, is the zero strain total energy and C_{ij} are the second order elastic constants.

As noted above, the elastic stiffness coefficients C_{ij} can be obtained by straining the lattice. According to the symmetry of the cubic crystal, it is completely described by three independent constants, C_{11}, C_{12}, and C_{44}, obtained by the three strains C1, C2, and C3 given below, respectively.

$$C1=\begin{pmatrix}\delta & 0 & 0\\ 0 & \delta & 0\\ 0 & 0 & \delta\end{pmatrix},\ C2=\begin{pmatrix}\delta & 0 & 0\\ 0 & -\delta & 0\\ 0 & 0 & \frac{\delta^2}{1-\delta^2}\end{pmatrix},\ C3=\begin{pmatrix}\frac{\delta^2}{1-\delta^2} & 0 & 0\\ 0 & 0 & \delta\\ 0 & \delta & 0\end{pmatrix} \tag{5}$$

The calculations of the elastic properties of the tetragonal structures are continued according to the symmetry of the tetragonal crystal using linear response theory performing six finite distortions of the lattice; it is completely described by six independent constants given in Table 3.

Table 3. The calculated elastic constants (C_{ij} in GPa) for 6–15 mol% doped yttria-stabilized zirconia with linear response theory.

Structure	C_{11}	C_{12}	C_{13}	C_{33}	C_{44}	C_{66}	B	G	E	υ
$Y_2Zr_6O_{15}$ (14.28 mol%)	433.37	115.78	114.48	451.77	66.35	78.60	223.21	98.85	258.41	0.31
$Y_2Zr_{14}O_{31}$ (6.67 mol%)	507.08	107.35	102.61	518.91	72.13	73.40	239.79	111.29	289.14	0.29
$Y_6Zr_{26}O_{61}$ (10.24 mol%)	493.15	103.50	106.24	484.22	62.17	59.70	233.61	99.03	260.32	0.31

The mechanical stability criteria for cubic and tetragonal structures are given as

$$C_{11}-C_{12}>0,\quad C_{44}>0,\quad C_{11}+2C_{12}>0 \tag{6}$$

$$C_{11}>0,\quad C_{33}>0,\quad C_{44}>0,\quad C_{66}>0,\quad C_{11}-C_{12}>0,\quad C_{11}+C_{33}-2C_{13}>0,$$
$$[2(C_{11}+C_{12})+C_{33}+4C_{13}]>0$$

As described below, we have also calculated bulk modulus (B) and shear modulus (G) for cubic and tetragonal structures from anisotropic elastic constants given as follows:

Cubic structure

$$B_V=B_R=(C_{11}+2C_{12})/3,$$

$$G_V=(C_{11}-C_{12}+3C_{44})/5,$$

$$G_R=5\,(C_{11}-C_{12})\,C_{44}/(4C_{44}+3(C_{11}-C_{12})),$$

Tetragonal structure

$$B_V=\frac{1}{9}\,[2C_{11}+C_{12})+C_{33}+4C_{13}] \tag{7}$$

$$B_R=\frac{(C_{11}+C_{12})\,C_{33}-2C_{13}^2}{C_{11}+C_{12}+2C_{33}-4C_{13}}$$

$$G_V = \frac{1}{30}\left[4C_{11} - 2C_{12} - 4C_{13} + 2C_{33} + 12C_{44} + 6C_{66}\right]$$

$$G_R = 15\left[\frac{18B_V}{(C_{11}+C_{12})C_{33} - 2C_{13}^2} + \frac{6}{C_{11}-C_{12}} + \frac{6}{C_{44}} + \frac{3}{C_{66}}\right]^{-1}$$

$$B = (1/2)(B_V + B_R),$$

$$G = (1/2)(G_V + G_R),$$

where the subscripts V and R stand for Voigt and Reuss forms, respectively.

Young's modulus E and Poisson's ratio υ are also obtained using

$$E = 9BG/(3B + G), \tag{8}$$

$$\upsilon = (3B - 2G)/[2x\,(3B + G)].$$

δ is strain parameter and $\delta = 0$ is referred to the equilibrium volume V_0 at 0 GPa. The strain parameter is varied from 0.07 to –0.07 in steps of 0.015 and the total energy is calculated at every single increment. A quadratic behavior in strain energy as a function of strain is used to determine the elastic modulus in Figure 4.

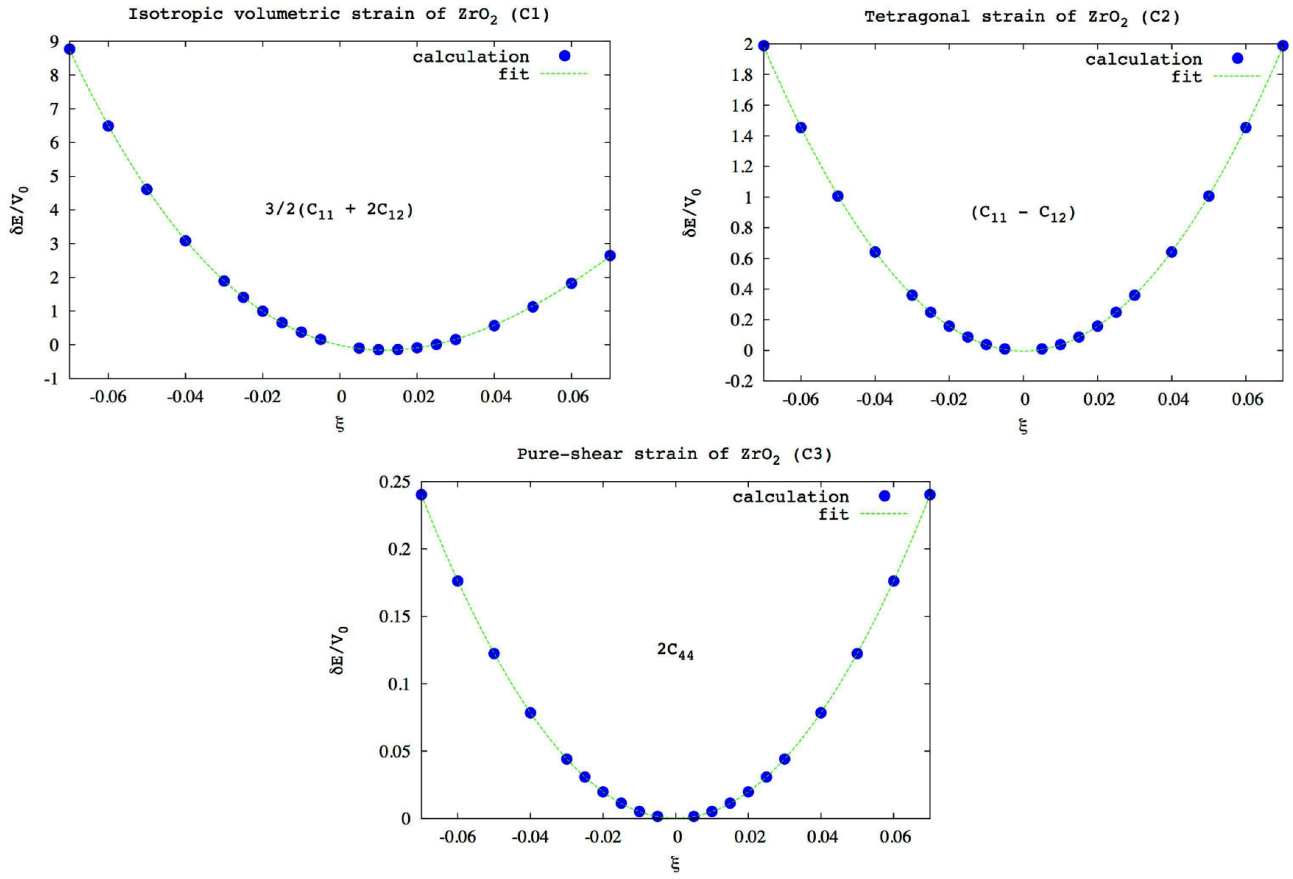

Figure 4. Changes in strain energy as a function of strain for cubic ZrO_2.

In addition to the structural and energetic stability, mechanical properties are determined in this study. Extensive systematic studies on the oxygen point defects in cubic ZrO_2 [9] exist, but similar studies are still lacking for yttria doped zirconia. In this study, we have shown the structural and mechanical properties of 6–15 mol% doped yttria-stabilized zirconia and they are mechanically stable. An understanding of the diffusion of oxygen vacancies with migration energy barriers is also essential for technological applications [20–23].

4. Summary and concluding remarks

Structural, energetic, and mechanical properties have been calculated for cubic zirconia and 6 mol% to 15 mol% doped yttria-stabilized zirconia within density functional theory. The physical parameters such as the energetics of formation and migration of oxygen vacancy also play important roles in oxides that are used in commercial and industrial applications. The calculated structural (lattice parameters, cell volume, bulk modulus, and derivative of bulk modulus) and elastic constants of structures studied here were in close agreement with experimental and theoretical values. Elastic properties have been calculated by using the strain-stress method and linear response theory in terms of first-principle calculations. We have created a yttria stabilized zirconia crystal structure from cubic zirconia. Because the crystallographic site of zirconium is replaced by yttrium atom, the crystal symmetry breaks. The cubic structure slightly deviates to a tetragonal structure. According to our result of similarity of C_{12} and C_{13}, C_{11} and C_{33}, and C_{44} and C_{66} for 6–15 mol % doped ytrria stabilized zirconia can be classified as a quasi-tetragonal structure. This aforementioned property can be used for future technological applications.

Acknowledgments

This work is also supported by Kırklareli University Research Project Unit (BAP) under Project No 125. Partial support for TÇ is provided by NSF EAGER and NSF IMI project.

References

[1] Fabbri, E.; Pergolesi, D.; Traversa, E. *Chem. Soc. Rev.* **2010**, *39*, 4355-4369.

[2] Fabbri, E.; Pergolesi, D.; Traversa, E. *Sci. Technol. Adv. Mater.* **2010**, *11*, 054503.

[3] Pergolesi, D.; Fabbri, E.; D'Epifanio, A. *Nature Materials* **2010**, *9*, 846-852.

[4] Dyer, C. K. *Sci. Am.* **1999**, *281*, 70.

[5] Andersen, N. H.; Clausen, K.; Hackett, M. A.; Hayes, W.; Hutchings M. T.; Macdonald, J. E.; Osborn, R. *Physica* **1986**, *136*, 315-317.

[6] Aldert, P.; Traverse, L. P. *J. Am. Ceram. Soc.* **1985**, *68*, 34.

[7] Stefanivich, E. V., Shluger, A. L., Catlow, C. R. A. *Phys. Rev. B* **1994**, *49*, 11560-11571.

[8] Jomard, G.; Petit, T.; Pasturel, A.; Magaud, L.; Kresse, G.; Hafner, J. *Phys. Rev. B* **1999**, *59*, 4044-4052.

[9] Malyi, O. I.; Wu, P.; Kulish, V.V.; Bai, K.; Chen, Z. *Solid State Ionics* **2012**, *212*, 117-122.

[10] Cousland, G. P.; Cui, X. Y.; Ringer, S.; Smith, A. E.; Stampfl, A. P. J.; Stampfl, C. M. *J. Phys. Chem. Solids* **2014**, *75*, 1252-1264.

[11] Pomfret, M. B.; Chad, S.; Varughese, B.; Walker, R. *Anal. Chem.* **2005**, *77*, 1791-1795.

[12] Liang, Z.; Wang, W.; Zhang, M.; Wu, F.; Chen, J. F.; Xue, C.; Zhao, H. *Physica B* **2017**, *511*, 10-19.

[13] Xu, Y. N.; Gu, Z. Q.; Ching, W. Y. *Phys. Rev. B* **1997**, *56*, 14993-15000.

[14] Kresse, G; Hafner, J. *Phys. Rev. B* **1993**, *47*, 558-561.

[15] Wyckoff, R. W. G. *Crystal Structures*, 2nd ed. Vol. 1; Interscience Publishers: New York, NY, USA, 1963.

[16] Ingel, R. P.; Lewis, D. III. *J. Am. Ceram. Soc.* **1988**, *71*, 265-271.

[17] Tian, D.; Zeng, C.; Wang, H.; Luo, H.; Cheng, X.; Xiang, C.; Wei, Y.; Li, K.; Zhu, X. *J. Alloy. Compd.* **2016**, *671*, 208-219.

[18] Zhao, X. S.; Shang, S. L.; Liu, Z. K.; Shen, J. Y. *J. Nucl. Mater.* **2011**, *415*, 13-17.

[19] Wu, Z.; Zhao, E. K.; Xiang, H.; Hao, X.; Liu, X.; Meng, J. *Physical Rev. B* **2007**, *56*, 54115-541130.

[20] Kandil, H. M.; Greiner, J. D.; Smith, J. F. *J. Am. Ceram. Soc.* **1984**, *67*, 341-346.

[21] Pace, N. G.; Saunders, GA.; Sumengen, Z.; Thorp, J. S. *J. Mater. Sci.* **1969**, *4*, 1106-1110.

[22] Lunt, A. J. G.; Xie, M. Y.; Baimpas, N.; Zhang, S. Y.; Kabra, S.; Kelleher, J.; Neo, T. K.; Korsunsky, A. M. *J. Appl. Phys.* **2014**, *116*, 053509-053517.

[23] Parkes, M.; Refson, K.; d'Avezac, M.; Offer, G. J.; Brandon, N. P.; Harrison, N. M. *J. Phys. Chem. A.* **2015**, *119*, 6412-6420.